Available online at www.sciencedirect.com
ScienceDirect
Journal of Hazardous Materials 144 (2007) 240–248
Journal of Hazardous Materials
www.elsevier.com/locate/jhazmat

# A combined electrocoagulation–sorption process applied to mixed industrial wastewater

Ivonne Linares-Hernández [a], Carlos Barrera-Díaz [a,*], Gabriela Roa-Morales [a], Bryan Bilyeu [b], Fernando Ureña-Núñez [c]

[a] *Universidad Autónoma del Estado de México, Facultad de Química, Paseo Colón intersección Paseo Tollocan S/N, C.P. 50120, Toluca, Estado de México, Mexico*
[b] *University of North Texas, Department of Materials Science and Engineering, PO Box 305310, Denton, TX 76203-5310, USA*
[c] *Instituto Nacional de Investigaciones Nucleares, A.P. 18-1027, Col. Escandón, Delegación Miguel Hidalgo, C.P. 11801, México, D.F., Mexico*

Received 3 June 2006; received in revised form 2 October 2006; accepted 7 October 2006
Available online 12 October 2006

**Abstract**

The removal of organic pollutants from a highly complex industrial wastewater by a aluminium electrocoagulation process coupled with biosorption was evaluated. Under optimal conditions of pH 8 and 45.45 A $m^{-2}$ current density, the electrochemical method yields a very effective reduction of all organic pollutants, this reduction was enhanced when the biosorption treatment was applied as a polishing step. Treatment reduced chemical oxygen demand (COD) by 84%, biochemical oxygen demand ($BOD_5$) by 78%, color by 97%, turbidity by 98% and fecal coliforms by 99%. The chemical species formed in aqueous solution were determined. The initial and final pollutant levels in the wastewater were monitored using UV–vis spectrometry and cyclic voltammetry. Finally, the morphology and elemental composition of the biosorbent was characterized with scanning electron microscopy (SEM) and energy dispersion spectra (EDS).


*Keywords:* Electrochemical process; Superfaradaic efficiencies; Biosorption; Industrial wastewater treatment

## 1. Introduction

Electrocoagulation is an electrochemical method of treating polluted water whereby sacrificial anodes dissolve due to a potential difference, producing active coagulant precursors (usually aluminum or iron ions). At the same time cathodic reactions occur, in many cases involving the evolution of hydrogen gas [1].

Recent research has shown that electrocoagulation is an effective technique for removing pollutants from lowland surface water [2], urban wastewaters [3] synthetic colloid-polluted wastes [4], restaurant effluents [5], metal plating wastes [6], and in actual industrial discharges [7,8]. The results from these studies show that this technique is one of the most promising methods for treating wastewater polluted with colloidal pollutants. Electrochemical methods offers two main advantages over traditional chemical treatment: less coagulant ion is required and less sludge is formed [2,3,6].

On the other hand, adsorption is a physicochemical wastewater treatment process, which is gaining prominence as a means of reducing metal ion concentrations in industrial effluents [9]. The biosorbents derived from dead biomass, are considered the cheapest and most abundant environmentally friendly option [10,11]. The development of inexpensive adsorbents for the treatment of wastewater is an important area in the environmental sciences [12,13]. However, raw biosorbents tend to leach large amounts of organic compounds during water treatment, as indicated by the green or yellow color of the water after biosorption [14]. In order to prevent this phenomenon, a biosorbent should be conditioned before its use.

The use of an electrochemical treatment as a pre-treatment step to enhance adsorption capability of biosorbents can be justified if the resulting wastewater quality expressed as color and COD removal is good. The techniques to be coupled must be carefully evaluated, because technical incompatibilities may

* Corresponding author. Tel.: +52 722 2173890; fax: +52 722 2175109.
*E-mail address:* cbarrera@uaemex.mx (C. Barrera-Díaz).

0304-3894/$ – see front matter © 2006 Elsevier B.V. All rights reserved.
doi:10.1016/j.jhazmat.2006.10.015

arise. Thus, the coupling of electrochemical and sorption processes might prove a judicious choice for treating industrial wastewater with mixtures of different types of pollutants.

In this study an aluminium electrocoagulation process is coupled with a biosorption step to address limitations of treating mixed industry wastewater. The effectiveness of aluminum electrocoagulation before and after a biological reactor, and the influence of different operating parameters were evaluated and optimized. Then, the electrochemically treated water is polished using biosorption. The selected biosorbent is *Ectodemis* of *Opuntia*, which is chemically conditioned prior its use. This biosorbent has been shown to be effective in improving water quality, particularly in removing metal ions [15]. Raw and treated wastewater was characterized by UV–vis spectroscopy and cyclic voltammetry. The physicochemical characteristics of the wastewater before and after applying the electrochemical + biosorption treatment are presented. The combined treatment reduced chemical oxygen demand (COD) by 84%, biochemical oxygen demand ($BOD_5$) by 78%, color by 97%, turbidity by 98% and Fecal Coliforms by 99%. Finally, the biosorbent morphology and composition was evaluated by scanning electron microscopy (SEM) and energy dispersion analysis (EDS).

## 2. Materials and methods

### 2.1. Wastewater samples

Samples of wastewater were collected from a treatment plant located at the end of an industrial park. This facility receives the industrial discharge of 144 different factories. Table 1 indicates the distribution and the nature of the wastewater that is being treated in the wastewater treatment plant.

All of the industrial effluents enter the wastewater treatment plant together. The plant has the following treatment operations: shredder, sand separator, oil and grease separator, primary clarifiers, biological activated sludge reactors, secondary clarifiers and chlorine disinfecting contact units. Influent and effluent samples were collected in plastic containers and cooled to 4 °C, then transported to the laboratory for analysis and electrochemical–sorption treatments.

Table 1
Companies that discharge effluents to the wastewater treatment plant

| Industrial sector | No. of companies |
|---|---|
| Chemical | 39 |
| Metal finishing | 34 |
| Textile | 22 |
| Food | 11 |
| Leather | 6 |
| Construction | 5 |
| Automotive | 4 |
| Pharmaceutical | 3 |
| Furniture | 3 |
| Plastics | 7 |
| Paints | 1 |
| Services | 9 |
| Total | 144 |

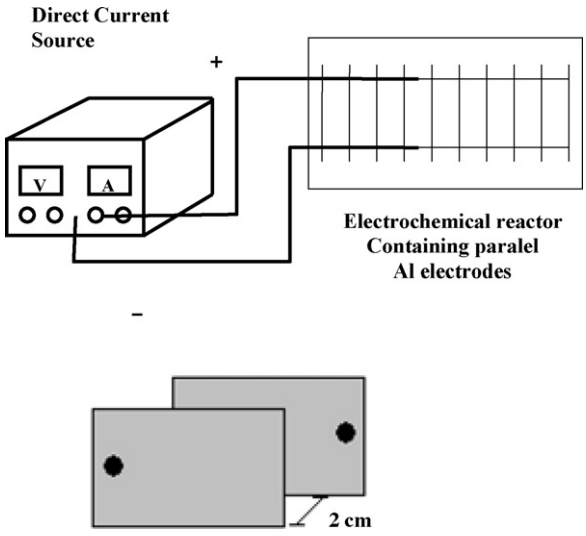


Fig. 1. A schematic diagram of the electrochemical reactor.

### 2.2. Electrochemical reactor

A batch electrochemical reactor was constructed for the electrocoagulation step. The electrode system is monopolar. The reactor cell contains an array of 10 parallel Al electrodes. Each electrode dimensions are 0.11 m long and 0.06 m wide. Each electrode has an area of 0.0132 $m^2$ for a total anodic surface, $A_a$ of 0.066 $m^2$. Each 4 $dm^3$ batch of water was treated in a bucket which served as the supply vessel for the reactor. A dc power source supplied the system with 1–4 A at 13 V, corresponding to a current density of 15.15–60.60 A $m^{-2}$. Fig. 1 shows a schematic diagram of the electrochemical reactor.

### 2.3. Conditioning of Ectodermis of Opuntia

The *Ectodermis* of *Opuntia* was collected from the city of Toluca in the central part of the state of México. The raw material was rinsed with distilled water; sun-dried for 5 days, then dehydrated at 80 °C for 48 h. Once the biomass cooled, it was crushed, milled and sieved through a no. 40 mesh. Thereafter, the material was stored in a desiccator. The main goal of using the biomass is to eliminate or reduce the color present in wastewater; therefore, this material needs conditioning to prevent leaching of colored organic components of the material itself during batch contact experiments [14]. In order to condition the biomass, the *Ectodermis* of *Opuntia* was treated with concentrated $H_2SO_4$ in a weight ratio of 1:1.8 peel to acid for 6 h at 160 °C. The acid-treated biomaterial was rinsed with deionized water several times and then dried at 105 °C for 6 h [15,16].

### 2.4. Methods of analysis

The initial evaluation of the electrochemical and sorption treatments was determined by analysis of the COD and color

(Pt/Co scale) at different time intervals. However, once the optimal conditions were found the raw and treated wastewater samples were analyzed using the $BOD_5$ and COD, aluminum content, pH, total coliforms and turbidity, as indicated in the Standard Methods procedures [17].

### 2.5. Cyclic voltammetric measurements

Cyclic voltammetry of crude and treated wastewater was performed using a standard three-electrode cell. The waveforms were generated by a potentiostat model BAS-100 W, controlled by BAS software. The carbon paste electrodes (CPE) were circular with a surface area of about 3.5 $mm^2$. The CPE was prepared from a 1:1 mixture of 99.99% pure single crystal graphite (Alfa AESAR) and nujol oil (Fluka). The paste was transferred into a PVC tube and compacted to eliminate trapped air then a copper conductor was inserted before the paste set. The surface of the electrode was renovated after each potential scan [18]. The scan rate was 100 mV $s^{-1}$. The reference electrode was an Ag/AgCl saturated with KCl and the counter electrode was a platinum wire.

### 2.6. Batch contact experiments

Adsorption studies were carried out by batch technique to obtain rate and equilibrium data following a previously proposed methodology [19,20]. A series of test tubes containing equal 10 mL volumes of adsorbate solutions of varying concentration were employed, at the resulting electrochemical treated wastewater pH (8). A known amount of adsorbent (0.1 or 0.05 g) was added into each test tube and agitated intermittently from 5 min to 24 h. Adsorption increased with increasing mixing time to a maximum at 0.5 h. Shaking for anytime between 1 and 24 h gave practically the same uptake.

The adsorbent material was dried and characterized using SEM, while the aqueous supernatant was analyzed for color and COD concentration using the previously described methods. All experiments were replicated.

### 2.7. UV–vis spectrometry

UV–vis spectra were obtained from samples of raw and treated wastewater using a double beam Perkin-Elmer 25 spectrophotometer. The scan rate was 960 nm $s^{-1}$ within the 900–200 nm wavelength range. The samples were scanned in quartz cells with a 1 cm optical path.

### 2.8. Biomass characterization

The raw and conditioned biomass samples were analyzed by scanning electron microscopy (SEM) and X-ray microanalysis. The analysis was performed on a Phillips XL-30 microscope to observe the composition and configuration of the structure. SEM provides images of rough material with resolution down to fractions of a micrometer, while energy disperse X-ray spectroscopy offers *in situ* elemental analysis.

### 2.9. Thermodynamic analysis

The existence of Al(III) complexes in aqueous solution has been reported [21,22]. Using this information the distribution diagrams of chemical species were calculated using the MEDUSA program [23].

## 3. Results

### 3.1. Actual performance of the wastewater treatment plant

The actual wastewater treatment plant consists of shredders, sand separators, oil and grease separators, primary clarifiers, biological activated sludge reactors, secondary clarifiers and a chlorine disinfecting unit. The COD and $BOD_5$ values are high, with a yearly average of 3500 and 1300 mg $dm^{-3}$, respectively. The actual treatment reduces these values by 60%, which still does not comply with environmental discharge standards. Thus, additional techniques are needed to improve the quality of the water.

In this study, we focus on treating wastewater at the inlet (IB) and outlet (OB) of the biological reactor. Table 2 shows the physicochemical characteristic of the actual treated wastewater.

Note that although the actual biological treatment reduces the $BOD_5$ by around 60%, other parameters such as the COD, color, turbidity and total solids still remain high. The BOD/COD ratio of wastewater entering the biological reactor is around 0.372, improving to 0.294 after the treatment. These results indicate that applying a biological method alone to treat this wastewater is not very effective, supporting the need for alternative methods.

### 3.2. Preliminary effect on the wastewater electrocoagulation at different pH conditions

Wastewater samples were taken from the inlet and outlet of the biological treatment tank, then electrochemically treated using the reactor described earlier, adjusting the pH (using NaOH or $H_2SO_4$) and applying 3 A of current. Tables 3 and 4 show the COD removal as a function of treatment time at different initial wastewater pH values.

Tables 3 and 4 show the maximum COD removal occurs in the pH range of 6–8. In both cases a reduction of the COD is observed beyond pH 10. These results agree with previous research, which indicates that the maximum COD removal in oil and grease contaminated restaurant wastewater is observed

Table 2
Selected properties of wastewater at the inlet and outlet of the biological reactor

| Parameter | IB | OB |
|---|---|---|
| COD (mg $dm^{-3}$) | 1700–2500 | 800–1267 |
| $BOD_5$ (mg $dm^{-3}$) | 930 | 373 |
| Color (Pt–Co U) | 2500–4750 | 1500–2500 |
| Turbidity (NTU) | 1400 | 900 |
| pH | 8 | 8.3 |
| Fecal coliforms, MPN (mg $dm^{-3}$) | 110,000 | 55,000 |
| Total solids (mg $dm^{-3}$) | 5360 | 4820 |

Table 3
COD removal from IB wastewater at different pH

| Time (min) | pH 2 | pH 4 | pH 6 | pH 8 | pH 10 | pH 12 |
|---|---|---|---|---|---|---|
| COD at different wastewater pH (mg dm$^{-3}$) | | | | | | |
| 0 | 1910 | 1910 | 1910 | 1920 | 1920 | 1930 |
| 10 | 1570 | 1290 | 1270 | 1260 | 1580 | 1680 |
| 20 | 1300 | 1100 | 1090 | 1080 | 1420 | 1650 |
| 30 | 1200 | 1100 | 1080 | 1060 | 1290 | 1600 |
| 40 | 1150 | 1060 | 1070 | 1040 | 1250 | 1580 |
| 50 | 1120 | 1050 | 1060 | 1040 | 1220 | 1540 |
| 60 | 1100 | 1040 | 1030 | 1030 | 1200 | 1530 |
| Removal (%) | 42.41 | 45.55 | 46.07 | 46.35 | 37.50 | 20.73 |

Table 4
COD removal from OB wastewater at different pH

| Time (min) | pH 2 | pH 4 | pH 6 | pH 8 | pH 10 | pH 12 |
|---|---|---|---|---|---|---|
| COD at different wastewater pH (mg dm$^{-3}$) | | | | | | |
| 0 | 1000 | 1020 | 1010 | 980 | 890 | 970 |
| 10 | 640 | 630 | 610 | 510 | 660 | 790 |
| 20 | 490 | 450 | 400 | 370 | 520 | 650 |
| 30 | 380 | 360 | 360 | 310 | 390 | 490 |
| 40 | 350 | 340 | 340 | 290 | 380 | 470 |
| 50 | 320 | 300 | 310 | 260 | 350 | 450 |
| 60 | 300 | 290 | 280 | 250 | 340 | 420 |
| Removal (%) | 70.00 | 71.57 | 72.28 | 74.49 | 61.80 | 56.70 |

around pH 7; the pH effect in the COD removal is not very significant in the pH range of 3–10. Nevertheless, COD removal dropped dramatically at pH values larger than 10 [5].

The pH in the COD removal in the range of 3–10 is not significant since the predominant aluminum chemical specie in this range is $Al(OH)_{3(s)}$ as can be observed in Fig. 2. However, it is interesting to note in Fig. 2 that at pH greater than 10 there is the presence of a new aluminum chemical specie in the system. This chemical specie $Al(OH)_4$ is soluble an directly affects the pollutant removal. The electrocoagulation mechanisms are explained in Section 3.5.

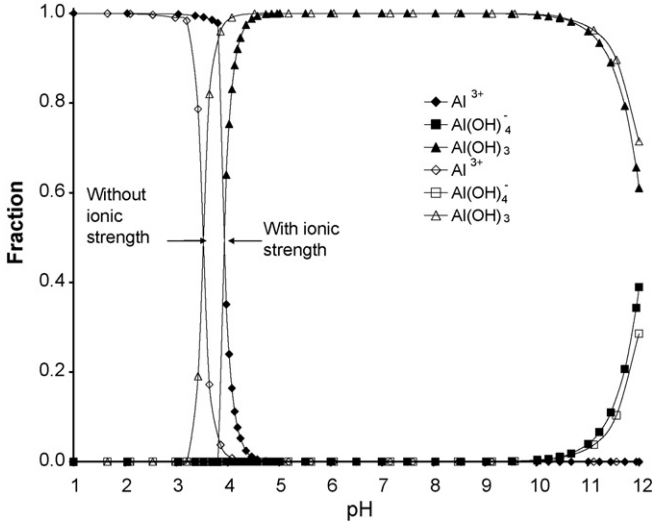


Fig. 2. Aluminum species distribution in wastewater as a function of pH. The influence of the ionic strength is to displace to the right the Al species distribution on wastewater.

Table 5
Pollutant reduction using different current densities

| Time (min) | Current density (A m$^{-2}$) | | | |
|---|---|---|---|---|
| | 15.15 | 30.3 | 45.45 | 60.6 |
| 0 | 1910 | 1910 | 1910 | 1910 |
| 10 | 1482 | 1421 | 1379 | 1364 |
| 20 | 1158 | 1126 | 1119 | 1103 |
| 30 | 1134 | 1080 | 1051 | 1012 |
| 40 | 1065 | 1057 | 1040 | 1012 |
| 50 | 1053 | 1046 | 1006 | 966 |
| 60 | 1053 | 1046 | 961 | 944 |
| Removal (%) | 44.80 | 45.20 | 49.70 | 50.50 |

Table 6
IB and OB pollutant reduction using aluminum electrocoagulation

| Parameter | Initial | IB | IB (removal, %) | OB | OB (removal, %) |
|---|---|---|---|---|---|
| COD (mg/dm$^{-3}$) | 1910 | 940.5 | 50.8 | 233.5 | 87.8 |
| Color | 4800 | 825 | 82 | 725 | 84.9 |
| Turbidity (NTU) | 1975 | 700 | 69.6 | 500 | 74.7 |

### 3.3. Optimum conditions applied to wastewater

As previously discussed, COD removal is quite similar from pH 4 to 8. Since the actual pH of wastewater is around 8.0, further experiments were performed in this condition.

Table 5 shows the variation of the COD as a function of current density, note that the best removal rate is achieved under 45.45 A m$^{-2}$ and no significant increase in the COD removal is observed when the current density is increased to 60.6 A m$^{-2}$. Table 6 shows the COD, color a, color and turbidity removal at pH 8.0, with a current density of 45.45 A m$^{-2}$ for 60 min on the IB and OB wastewaters.

As shown in Table 6, the best removal rates are achieved using the wastewater that has been treated in the biological reactor. A detailed analysis of the treated wastewater is shown in Table 7.

It is important to note that not only has the COD content been diminished using the electrochemical treatment, but also the $BOD_5$. The fecal coliform concentration and color are also reduced by 99.8% and 70%, respectively. Similar behavior is

Table 7
Characteristics of the OB wastewater before and after electrocoagulation

| Parameter | OB wastewater | Electrochemically treated OB wastewater |
|---|---|---|
| COD (mg dm$^{-3}$) | 1176 | 392 |
| $BOD_5$ (mg dm$^{-3}$) | 373 | 147 |
| Color (Pt–Co U) | 2500 | 750 |
| Conductivity (S cm) | 58,800 | 37,600 |
| Turbidity (NTU) | 900 | 210 |
| pH | 8.4 | 9.6 |
| Fecal coliforms, MPN (mg dm$^{-3}$) | 55,000 | >3 |
| Aluminum (mg dm$^{-3}$) | 1.0 | 21.4 |

observed for other parameters. However, the treated water does have a higher concentration of aluminum.

### 3.4. Current efficiencies

The Al concentration in wastewater plays an important role in pollutant removal. Concentration and pH define the different possible Al chemical species present in aqueous solution. Using Faraday's law to calculate the maximum amount of Al produced in the electrochemical process in Eq. (1), with the experimental conditions of 3 A of current and 60 min of electrolysis along with the Faraday constant ($F$ 96 500 C mol$^{-1}$) and the charge on the cation ($z$ = +3), it is possible to calculate the maximum amount of Al, in this case 0.036 mol or 972 mg:

$$n = \frac{It}{zF} \tag{1}$$

The Al concentration in solution can be calculated using Eq. (2):

$$[\mathrm{M}] = \frac{n}{V} \tag{2}$$

where $n$ is the number of moles and $V$ is the volume (4 dm$^{-3}$) of the reactor. The maximum Al concentration is thus 242 mg dm$^{-3}$.

A particular effect that has been recently noted is the so-called "superfaradaic efficiencies". This term describes the difference between the theoretical amount of aluminum in aqueous solution and the actual Al detected. The detected Al concentration in aqueous solution in the mixed solution is 558 mg dm$^{-3}$ (previous to settling). The theoretical calculation corresponds to 242 mg dm$^{-3}$, this implies that there is an excess of 230%.

A possible explanation of this difference is that a chemical process takes place at the cathode promoting aluminum dissolution. The electrochemical oxidation and reduction of water can modify the pH on the anode and cathode surfaces with respect to the bulk pH. This is especially important on the cathode, where the pH can become strongly alkaline. This can justify the important contribution of the aluminum chemical dissolution in the cathode to the total dissolution rate [4].

### 3.5. Electrocoagulation mechanisms

The chemical dissolution process corresponds to the oxidation of the aluminum sheets with the simultaneous reduction of water to form hydrogen [24], as shown in Eq. (3):

$$2\mathrm{Al}_{(s)} + 6\mathrm{H_2O} \rightarrow 2\mathrm{Al}_{(aq)}{}^{3+} + 3\mathrm{H}_{2(g)} + 6\mathrm{OH}_{(aq)}{}^{-} \tag{3}$$

On the other hand, the electrochemical processes that occur on the anode and on the cathode surfaces are represented in Eqs. (4)–(6). On the anode, aluminum dissolution and oxygen evolution can compete. On the cathode, hydrogen evolution is the main expected reaction. Hydrogen is generated in both the chemical and the electrochemical processes:

$$\mathrm{Al}_{(s)} \rightarrow \mathrm{Al}_{(aq)}{}^{3+} + 3\mathrm{e}^{-} \tag{4}$$

$$2\mathrm{H_2O} \rightarrow \mathrm{O}_{2(g)} + 4\mathrm{H}_{(aq)}{}^{+} + 4\mathrm{e}^{-} \tag{5}$$

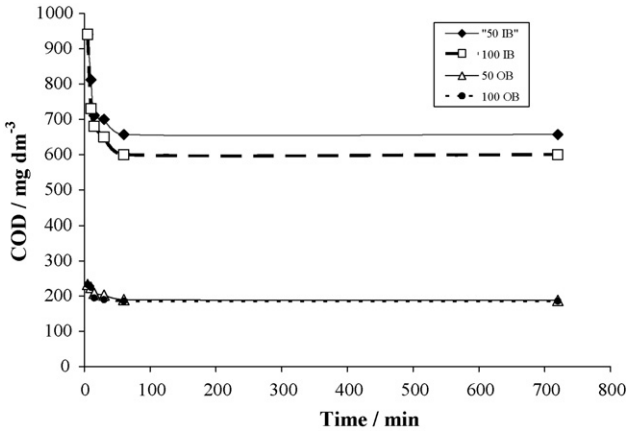


Fig. 3. COD biosorption kinetics using the electrochemically treated wastewater from the inlet of the biological reactor (IB) and the outlet of the biological reactor (OB) at different doses of the treated *Ectodermis* of *Opuntia* (50 and 100 mg).

$$\mathrm{H_2O} + \mathrm{e}^{-} \rightarrow (1/2)\mathrm{H}_{2(g)} + \mathrm{OH}_{(aq)}{}^{-} \tag{6}$$

The aluminum and hydroxide ions are expected to form $\mathrm{Al(OH)}_{3(s)}$.

Once the aluminum is dissolved (chemically or electrochemically), different aluminum species can be formed, depending on the pH of the solution and the presence of other ions in the aqueous media. In Fig. 2, the distribution of aluminum species in the actual solution taking into account the influence of the ionic strength is shown as a function of pH.

### 3.6. Energy consumption

Once that the required volts are obtained and from the experimental test and the optimal current is know then is possible to estimate the amount of Watts required as shown in

$$\mathrm{Watt} = \mathrm{V} \times \mathrm{A} \tag{7}$$

In our experimental conditions:

$$\mathrm{Watt} = 45.45\ \mathrm{A\,m^{-2}} \times 3\ \mathrm{V} = 136.35$$

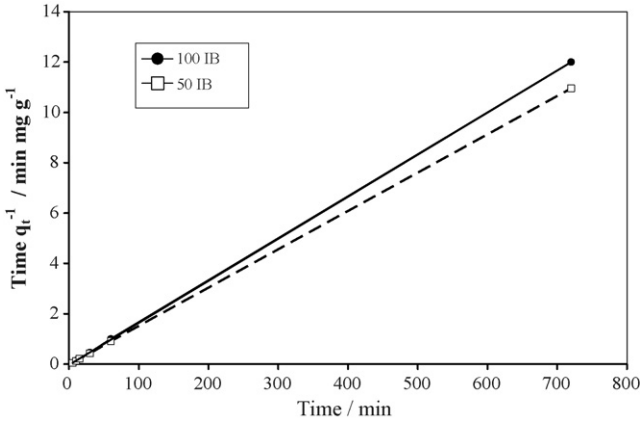


Fig. 4. Bisorption kinetic data fitted to a pseudo-second-order model from the Inlet of the Biological reactor (IB) at different doses of the treated *Ectodermis* of *Opuntia* 50 (□) and 100 mg (●).

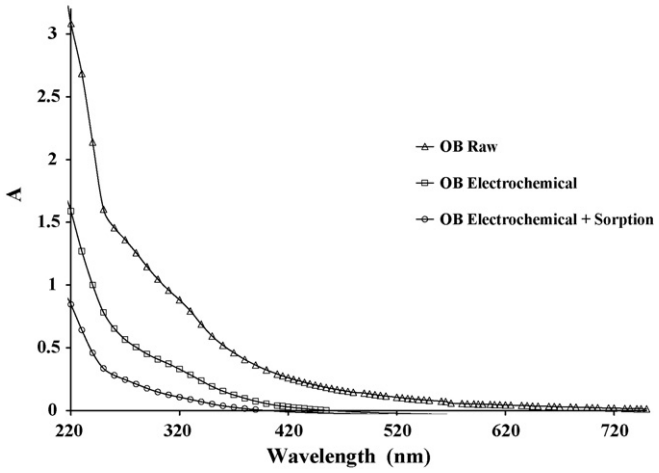


Fig. 5. UV–vis spectra of the raw outlet of the biological reactor wastewater, the electrochemically treated water and water after the electrochemically + sorption treatment.

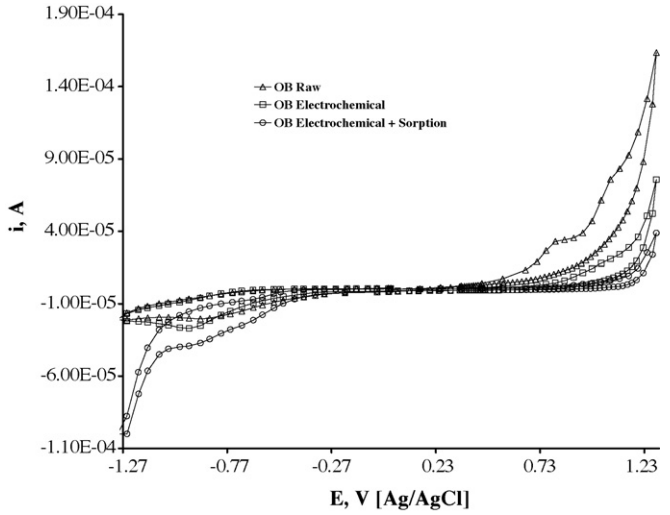


Fig. 6. Cyclic voltammograms recorded at the 3.5 mm$^2$ CPE over the potential window from −1.3 to 1.2 V of the raw OB, electrolytic treated and electrochemical + sorption treated wastewater at a scan rate of 0.1 V s$^{-1}$.

Then, this quantity should be converted in kWh dividing by 1000 and multiplying for the process time, which results in 8.181 kWh. In this way it is obtained the total amount of energy required for the electrolysis. At this time the cost of 1 kWh in USA is 8.39 cents/kWh it gives 68.6 cents [25].

### 3.7. Biosorption kinetics

Fig. 3 shows the COD adsorption kinetics of the electrochemically treated wastewater from the inlet and the outlet of the biological reactor. It also shows the effect of different quantities of biomass. The initial decrease in COD occurred rapidly in all cases, with no additional changes over longer periods of time. Larger COD decreases were observed in the IB wastewater during the first 100 min of contact time. Biosorption in both IB and OB reached equilibrium in 100 min. The equilibrium COD uptake was 30–35% in the IB wastewater, whereas a 5–20% COD removal was observed for the OB wastewater. After the equilibrium time of 100 min, no more COD was absorbed for any wastewater suggesting that the available sites on the biosorbent are the limiting factor.

Different mathematical models were employed to fit the experimental data, for all cases, a pseudo-second-order describes the process. The pseudo-second-order equation can be written as

$$\frac{dq_t}{dt} = k_2(q_e - q_t) \tag{8}$$

where $k_2$ (g mg$^{-1}$ min$^{-1}$) is the rate constant. Integration of this equation and rearranging in a linear form gives

$$\frac{t}{q_t} = \frac{1}{k_2 q_e^2} + \frac{1}{q_e}t \tag{9}$$

Table 8
A comparison of the Freundlich and Langmuir adsorption constants obtained from the Freundlich and Langmuir adsorption isotherms of IB and OB wastewater

| Wastewater | Langmuir | | | Freundlich | | |
|---|---|---|---|---|---|---|
| | $Q^0$ (mg L$^{-1}$) | $K_L$ (L mg$^{-1}$) | $r^2$ | $K_F$ (mg g$^{-1}$) | 1/$n$ | $r^2$ |
| IB | 4.0 | 0.184 | 0.993 | 1.1 | 0.140 | 0.854 |
| OB | 2.0 | 0.344 | 0.997 | 1.11 | 0.313 | 0.852 |

Table 9
Characteristics of the raw OB wastewater before and after applying the electrochemical + biosorption treatment

| Parameter | OB wastewater | Electrochemical + biosorption treated OB wastewater | Global efficiency removal (%) |
|---|---|---|---|
| COD (mg dm$^{-3}$) | 1176 | 187 | 84 |
| $BOD_5$ (mg dm$^{-3}$) | 373 | 82 | 78 |
| Color (Pt–Co U) | 2500 | 75 | 97 |
| Conductivity (S cm) | 58,800 | 23,400 | 60.2 |
| Turbidity (NTU) | 900 | 10 | 98.8 |
| pH | 8.4 | 9.6 | – |
| Fecal coliforms, MPN (mg dm$^{-3}$) | 55,000 | >3 | 99.9 |
| Aluminum (mg dm$^{-3}$) | >1.0 | >1.0 | – |

Fig. 4 shows the pseudo-second-order kinetic regime, associated with the COD sorption at the inlet of the biological reactor using the *Ectodermis* of *Opuntia*: it can be observed that the model describes the experimental behavior. The rate constant for 100 IB is 0.0167 and 0.0153 for 50 IB. Similar results were obtained for the sorption of metal ions in *Ectodermis* of *Opuntia*, the removal of nickel using wine processing waste sludge and removal of dyes using dried activated sludge [26–28].

The adsorption constants evaluated from the linearized Freundlich and Langmuir adsorption isotherms of COD are presented in Table 8. The Langmuir and Freundlich constants were used to compare the biosorption capacity of the *Ectodermis* of *Opuntia*. From Table 8, very high regression correlation coefficients (>0.99) were found for the Langmuir model. This suggests that the Langmuir model is suitable for describing the biosorption equilibrium from the IB and OB wastewater. The values of $Q^0$ found in this study are similar to the $Q^0$ obtained when wine processing waste sludge was used for pollutant removal [27].

### 3.8. Electrochemical + sorption treatment

Table 9 shows the physicochemical characteristics of the OB wastewater and the results obtained when the coupled treatment is applied to this wastewater. Note the effectiveness of the coupled treatment in pollutant removal.

### 3.9. UV–vis spectra

The UV–vis spectra of the raw, electrochemically and sorption treated wastewater are shown in Fig. 5. There is a continuous signal curve in the region around 220–420 nm in the spectra corresponding to components of the wastewater. It is interesting that

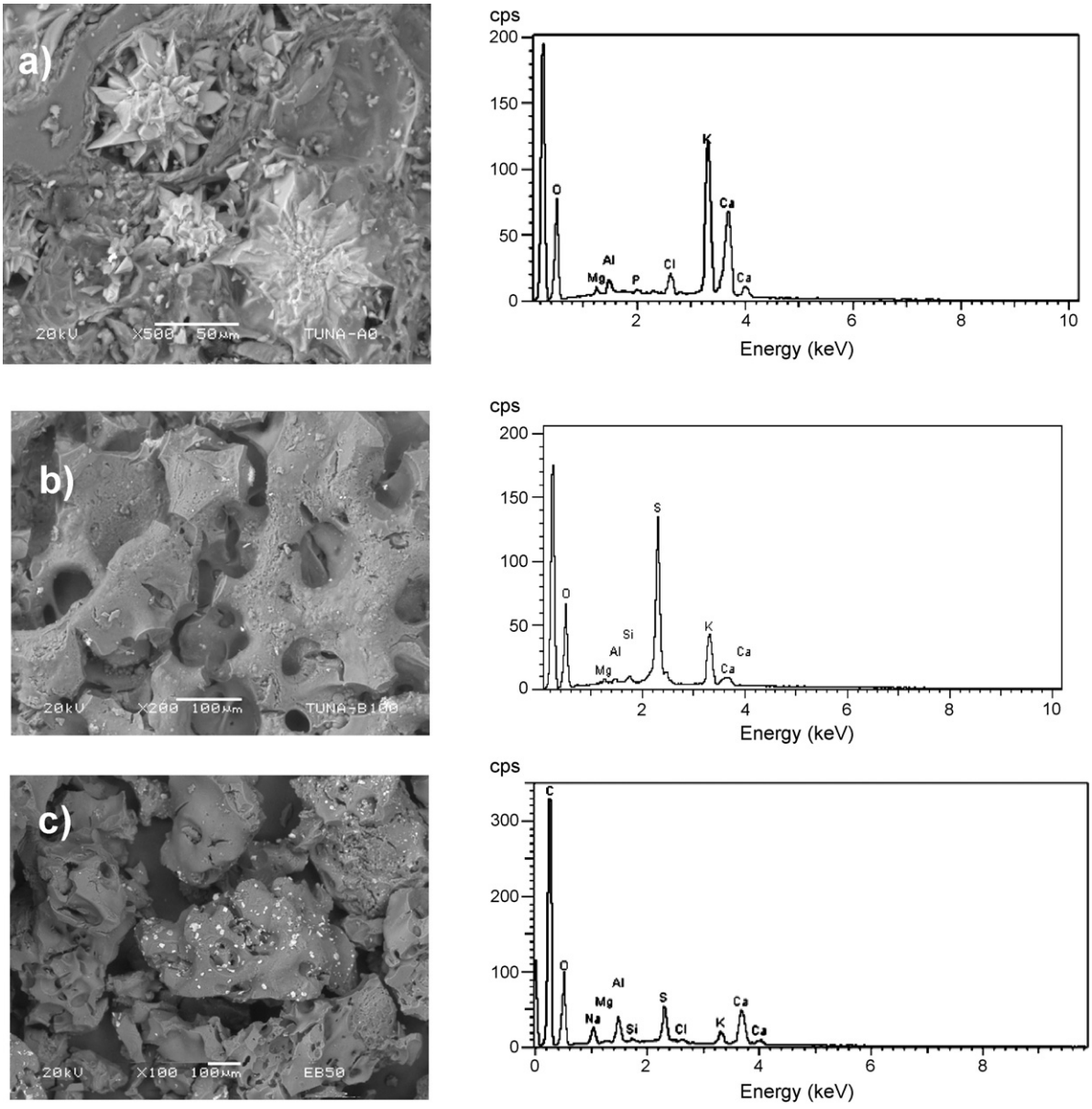


Fig. 7. Micrograph of the natural (a), conditioned (b), and used (c) *Ectodermis* of *Opuntia*. The photographs were recorded at the indicated magnification.

the intensity of the curves decrease as electrochemical and sorption treatments are applied. The peak around 220 nm decreases by 50% when electrochemical treatment is applied (absorbance decreases from 3.3 to 1.6) and by 70% using further sorption treatment. These results indicate that there is a significant color reduction of the raw wastewater when the electrochemical and sorption treatments are both applied. Color removal is associated with both electrocoagulation and biosorption processes that are taking place when the combined treatment is carried out.

### 3.10. Cyclic voltammetry

To determine the electrochemical characteristics of the raw and treated wastewater, and processes occurring at the electrodes, a series of cyclic voltammetry experiments were performed using a CPE as the working electrode. Cyclic voltammetry results indicate that a chemically irreversible oxidation peak in the wastewater is detectable at potentials lower that those corresponding to oxygen evolution as shown in Fig. 6. This peak corresponds to the direct electrochemical oxidation of pollutants present in wastewater. It is important to note that when cyclic voltammetry is applied after wastewater is electrochemically treated, the peak does not appear in the voltammogram indicating that pollutants in the solution have been oxidized. Thus, these voltammograms clearly indicate that there are processes attributable to direct oxidation of pollutants and these phenomena contribute to the destruction of organic matter present in the solution, when electrochemical treatment is applied and no other organic pollutants are introduced into the biosorption treated wastewater. Finally, this study confirms that wastewater quality is improved using the electrochemical biosorption treatment.

### 3.11. Scanning electron microscopy microphotographs

SEM and EDS provides information about the morphology and elemental composition of the *Ectodermis* of *Opuntia* in its natural, chemically treated and post-sorption states. The microphotographs in Fig. 7 show different morphological images of the *Ectodermis* of *Opuntia*. In Fig. 7a the *Ectodermis* of *Opuntia* presents a continuous structure with Ca and K needle-like structures on the surface. When the biosorbent is chemically modified with $H_2SO_4$, the morphology changes into the porous structure in Fig. 7b. Finally, when the biosorbent is added to treated wastewater in Fig. 7c, bright points appear on the surface indicating that Al metal has been sorbed. This technique also allows elemental analysis of the sample, as shown in Fig. 7. The peaks in Fig. 7a indicate that carbon, oxygen, calcium and potassium are the main elements present in the natural *Ectodermis* of *Opuntia*. After the chemical conditioning, the peak intensities of Ca and K decrease and S is detected (Fig. 7b). The used biosorbent has aluminum particles generated by the electrolysis (Fig. 7c).

## 4. Conclusions

The proposed electrochemical + sorption method used in this study reduces the concentration of pollutants in industrial wastewater. Cyclic voltammetry and UV–vis spectroscopy confirm the improvement in the wastewater quality and removal of pollutants by the coupled treatment. Finally, the morphology of the biosorbent is revealed by scanning electron microscopy and the presence of carbon, oxygen, aluminum and sulfur in this sorbent is confirmed by elemental analysis.

## Acknowledgements

The authors wish to acknowledge the support given by the Universidad Autónoma del Estado de Mexico, specifically the Facultad de Química (Project UAEM 2228/2006). Support from CONACYT and supporting research by SNI are greatly appreciated.

## References

[1] P.K. Holt, G.W. Barton, C.A. Mitchell, The future of electrocoagulation as a localized water treatment technology, Chemosphere 59 (3) (2005) 355–367.
[2] J.Q. Jiang, N. Graham, C.A. André, G.H. Kelsall, N. Brandon, Laboratory study of electro-coagulation-flotation for water treatment, Water Res. 36 (16) (2002) 4064–4078.
[3] E. Vik, D.A. Carlson, A.S. Eikum, E.T. Gjessing, Electrocoagulation of potable water, Water Res. 18 (11) (1984) 1335–1360.
[4] P. Cañizares, F. Martínez, M. Carmona, J. Lobato, M.A. Rodrigo, Continuous electrocoagulation of synthetic colloid-polluted wastes, Ind. Eng. Chem. Res. 44 (22) (2005) 8171–8177.
[5] G. Chen, X. Chen, P.L. Yue, Separation of pollutants from restaurant wastewater by electrocoagulation, Sep. Purif. Technol. 19 (2000) 65–76.
[6] C. Barrera-Díaz, M. Palomar-Pardavé, M. Romero-Romo, S. Martínez, Chemical and electrochemical considerations on the removal process of hexavalent chromium from aqueous media, J. Appl. Electrochem. 33 (2003) 61–71.
[7] C. Barrera-Díaz, F. Ureña-Nuñez, E. Campos, M. Palomar-Pardavé, M. Romero-Romo, A combined electrochemical–irradiation treatment of highly colored and polluted industrial wastewater, Radiat. Phys. Chem. 67 (2003) 657–663.
[8] C. Barrera-Díaz, G. Roa-Morales, L. Avila-Cordoba, T. Pavón-Silva, B. Bilyeu, Electrochemical treatment applied to food-processing industrial wastewater, Ind. Eng. Chem. Res. 45 (1) (2006) 34–38.
[9] K.K.H. Choy, J.F. Porter, G. McKay, Single and multicomponent equilibrium studies for the adsorption of acidic dyes on carbon from effluents, Langmuir 20 (22) (2004) 9646–9656.
[10] B. Nasernejad, T.E. Zadeh, P.B. Bonakdar, M.E. Bygi, A. Zamani, Comparison for biosorption modeling by heavy metals (Cr(III), Cu(II), Zn(II)) adsorption from wastewater by carrot residues, Process Biochem. 40 (2005) 1319–1322.
[11] L.K. Cabatingan, R.C. Agapay, J.L.L. Rakels, M. Ottens, L.A.M. Van der Wielen, Potential of biosorption for the recovery of chromate in industrial wastewaters, Ind. Eng. Chem. Res. 40 (10) (2001) 2302–2309.
[12] K. Wagner, S. Schulz, Adsorption of phenol, chlorophenols and dihydroxybenzenes onto unfunctionalized polymeric resins at temperatures from 294.14 K to 318.15 K, J. Chem. Eng. Data 46 (2001) 322–330.
[13] A.K. Jain, V.K. Gupta, S. Jain, Suhas, Removal of chlorophenols using industrial wastes, Environ. Sci. Technol. 38 (2004) 1195–1200.
[14] J.P. Chen, L. Yang, Chemical modification of *Sargassum* sp. for prevention of organic leaching and enhancement of uptake during metal biosorption, Ind. Eng. Chem. Res. 44 (26) (2005) 9931–9942.
[15] H. Barrera, F. Ureña-Nuñez, B. Bilyeu, C. Barrera-Díaz, Removal of chromium and toxic ions present in mine drainage by *Ectodermis* of *Opuntia.* J. Hazard. Mater., in press.
[16] B.S. Inbaraj, N. Sulochana, Carbonised jackfruit peel as an adsorbent for the removal of Cd(II) from aqueous solution, Bioresour. Technol. 94 (2004) 49–52.

[17] APHA, AWWA, Standard Methods for the Examination of Water and Wastewater, 19th ed., American Public Health Association, Washington, DC, 1995.
[18] G. Roa-Morales, L. Galicia, M.T. Ramírez-Silva, Evidence of ternary inclusion complexes formation using factorial design and determination of constant, J. Inc. Phenom. 46 (2003) 139–145.
[19] V.K. Gupta, M. Gupta, D. Sharma, Process development for the removal of lead and chromium from aqueous solutions using red mud—an aluminum industry waste, Water Res. 35 (5) (2001) 1125–1134.
[20] V.K. Gupta, S. Sharma, Removal of Zinc from aqueous solutions using baggase fly ash—a low cost adsorbent, Ind. Eng. Chem. Res. 42 (25) (2003) 6224–6619.
[21] M.R. Smith, A.E. Martell, Critical Stability Constants, Plenum Press, USA, 1974.
[22] C. Baes, R. Mesmer, The Hydrolysis of Cations, Robert E. Kriegeer, Malabar, FL, 1986.
[23] I. Puigdomenech, Hydrochemical Equilibrium Constants Database (MEDUSA), Royal Institute of Technology, Stockolm, 1997.
[24] T. Picard, G. Cathalifaud-Feuillade, M. Mazet, C. Vandensteendam, Cathodic dissolution in the electrocoagulation process using aluminium electrodes, J. Environ. Monit. 2 (2000) 77–80.
[25] http://www.eia.doe.gov/cneaf/electricity/epm/table5_3.html.
[26] C. Barrera-Díaz, C. Almaraz-Calderon, Ma.T. Olguín-Gutiérrez, M. Romero-Romo, M. Palomar-Pardavé, Environ. Technol. 26 (2005) 821–829.
[27] C. Liu, M. Kuang-Wang, Y. Li, Removal of nickel from aqueous solution using wine processing waste sludge, Ind. Eng. Chem. Res. 44 (5) (2005) 1438–1445.
[28] Z. Aksu, Biosorption of reactive dyes by dried activated sludge: equilibrium and kinetic modeling Biochem, Eng. J. 7 (2001) 79–84.